

# Density-equalizing map projections: Diffusion-based algorithm and applications

Michael T. Gastner and M. E. J. Newman

*Physics Department and Center for the Study of Complex Systems,,  
University of Michigan, Ann Arbor, MI 48109*

## **Abstract**

Map makers have for many years searched for a way to construct cartograms—maps in which the sizes of geographic regions such as countries or provinces appear in proportion to their population or some similar property. Such maps are invaluable for the representation of census results, election returns, disease incidence, and many other kinds of human data. Unfortunately, in order to scale regions and still have them fit together, one is normally forced to distort the regions' shapes, potentially resulting in maps that are difficult to read. Here we present a technique for making cartograms based on ideas borrowed from elementary physics that is conceptually simple and produces easily readable maps. We illustrate the method with applications to disease and homicide cases, energy consumption and production in the United States, and the geographical distribution of stories appearing in the news.

## 1 Introduction

Suppose we wish to represent on a map some data concerning, to take the most common example, the human population. For instance, we might wish to show votes in an election, incidence of a disease, number of cars, televisions, or phones in use, numbers of people falling in one group or another of the population, by age or income, or any other variable of statistical, medical, or demographic interest. The typical course under such circumstances would be to choose one of the standard (near-)equal-area projections for the region of interest and plot the data on it either as individual data points or using some sort of color code. The interpretation of such maps however can be problematic. A plot of disease cases, for instance, will inevitably show high incidence in cities and low incidence in rural areas, solely because there is a higher density of people living in cities. Figure 1(a), for example, shows the distribution of lung cancer cases among males in the state of New York between 1993 and 1997. Cases are particularly dense in New York City and its suburbs and sparse in the rural north of the state, but this could be purely a population effect and nothing to do with the disease itself.

To get a clearer impression of the situation we can instead plot a fractional measure of disease incidence rather than raw incidence data; we plot some measure of the number of cases per capita, binned in segments small enough to give good spatial resolution but large enough to give reliable sampling. Then we can use a color code to indicate different per capita rates on the map, as in Fig. 1(b). This procedure however has its own problems since it discards all information about where most of the cases are occurring. In Fig. 1(b), for example, there is now no way to tell that a large fraction of all cases occur in the New York City area.

Ideally, we would like some geographic representation of the data that allows us to see simultaneously where each individual case occurs as well as the per capita incidence. Though it appears at first that these two goals are irreconcilable, this is not in fact the case. On a normal area-preserving or approximately area-preserving projection, such as that used in Fig. (1), they are indeed irreconcilable. But if we can construct a projection in which areas

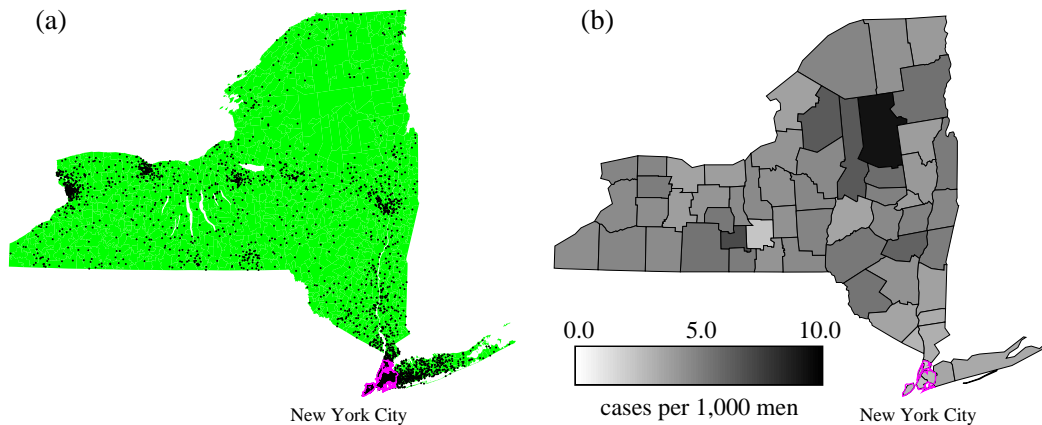


Figure 1: Lung cancer cases among males in the state of New York, 1993-1997. (a) Each dot represents 10 cases, randomly placed within the zip-code area of occurrence. Since there are 1598 zip codes in the state, each case can be located quite accurately. (Data from the New York State Department of Health.) (b) Incidence rates by county, 1992-1996.

on the map are proportional not to areas on the ground but instead to human population, then we can have our cake and eat it. Disease cases or other similar data plotted on such a projection will have the same density in areas with equal per capita incidence regardless of the population, since both the raw numbers of cases and the area will scale with the population. However, each case or group of cases can still be represented individually on such a map, so it will be clearly visible where most of the cases occur. Projections of this kind are known as value-by-area maps, density equalizing maps, anamorphoses, or cartograms [1, 2, 3, 4].

The construction of cartograms turns out to be a challenging undertaking. A variety of methods have been put forward, but none of them have been entirely satisfactory. In particular, they often produce highly distorted maps that are difficult to read or projections that are badly behaved under some circumstances, with overlapping regions or strong dependence on coordinate axes. In many cases the methods proposed are also computationally demanding, sometimes taking hours to produce a single map. Here we describe a new method based on the physics of diffusion which is, we believe, intuitive, while

also producing elegant, well-behaved, and useful cartograms whose calculation makes relatively low demands on our computational resources.

## 2 The diffusion cartogram

It is a trivial observation that on a true population cartogram the population is necessarily uniform: once the areas of regions have been scaled to be proportional to their population then, by definition, population *density* is the same everywhere. Thus, one way to create a cartogram given a particular population density is to allow population somehow to “flow away” from high-density areas into low-density ones until the density is equalized everywhere. This immediately brings to mind the diffusion process of elementary physics, and in fact it is not difficult to show that simple Fickian (or linear) diffusion achieves just such a density equalization. This is the basis for our method of constructing a cartogram.

We describe the population by a density function  $\rho(\mathbf{r}, t)$ , where  $\mathbf{r}$  represents geographic position and  $t$  time. At  $t = 0$  the population density is the one observed in reality, and then we allow this density to diffuse. The current density, measuring the amount and direction of flow, is given by

$$\mathbf{J} = \mathbf{v}(\mathbf{r}, t) \rho(\mathbf{r}, t), \quad (1)$$

where  $\mathbf{v}(\mathbf{r}, t)$  and  $\rho(\mathbf{r}, t)$  are the velocity and density respectively at position  $\mathbf{r}$  and time  $t$ . In Fickian diffusion the current density follows the gradient of the density field thus:

$$\mathbf{J} = -\nabla\rho, \quad (2)$$

meaning that the flow is always directed from regions of high density to regions of low density and will be faster when the gradient is steeper. Conventionally, there is a diffusion constant in Eq. (2) that sets the time scale of the diffusion process. But since we are only interested in the limit  $t \rightarrow \infty$  we can set this diffusion constant equal to one without loss of generality.

The diffusing population is conserved locally so that

$$\nabla \cdot \mathbf{J} + \frac{\partial \rho}{\partial t} = 0. \quad (3)$$

Combining Eqs. (1), (2), and (3) we then arrive at the familiar diffusion equation:

$$\nabla^2 \rho - \frac{\partial \rho}{\partial t} = 0 \quad (4)$$

and the expression for the velocity field in terms of the population density:

$$\mathbf{v}(\mathbf{r}, t) = -\frac{\nabla \rho}{\rho}. \quad (5)$$

The calculation of the cartogram involves solving Eq. (4) for  $\rho(\mathbf{r}, t)$  starting from the initial condition in which  $\rho$  is equal to the given population density of the region of interest and then calculating the corresponding velocity field from Eq. (5). The cumulative displacement  $\mathbf{r}(t)$  of any point on the map at time  $t$  can be calculated by integrating the velocity field thus:

$$\mathbf{r}(t) = \mathbf{r}(0) + \int_0^t \mathbf{v}(\mathbf{r}, t') dt'. \quad (6)$$

In the limit  $t \rightarrow \infty$  the set of such displacements for all points on the original map defines the cartogram.

Most of the time, we are not interested in mapping the entire globe, but only some part of it, which means that the area of interest will have boundaries (e.g., country borders or coastlines) beyond which we don't know or don't care about the population density. It would be inappropriate to represent the regions outside these boundaries as having zero population, even if they are, like the ocean, unpopulated, since this would cause arbitrary expansion of the cartogram as the population diffused into its uninhabited surroundings. (This is true of essentially all methods for constructing cartograms.) Instead, therefore, we apply a "neutral buoyancy" condition, floating the area of interest in a "sea" of uniform population density equal to the mean density of the map as a whole. This keeps the total area under consideration constant during the diffusion process.

The whole system, including the sea, is then enclosed in a box.<sup>1</sup> For sim-

---

<sup>1</sup>Note that we do not fix the shape of the borders or coastlines in our cartogram, as others have occasionally done. Doing so can create bottlenecks in the diffusion flow, which we avoid by allowing free motion of all points, whether they are near a border or not. Fixing external boundaries in fact often produces worse cartograms because it requires more substantial distortions of internal boundaries.

plicity we consider only rectangular boxes, as most others have done also.<sup>2</sup> Provided the dimensions  $L_x$  and  $L_y$  of the box are substantially larger than the area to be mapped, the dimensions themselves do not matter. In the limit  $L_x, L_y \rightarrow \infty$  the cartogram will be a unique deterministic mapping, independent of the coordinate system used, with no overlapping regions. In practice, we find that quite moderate system sizes are adequate—dimensions two to three times the linear extent of the area to be mapped appear to give good results. We also need to choose boundary conditions on the walls of the box. This choice too has no great effect on the results, provided the size of the box is reasonably generous. We use Neumann boundary conditions in which there is no flow of population through the walls of the box.

The considerations above completely specify our method and are intuitive and straightforward. The actual implementation of the method, if one wants a calculation that runs quickly, involves a little more work. We solve the diffusion equation in Fourier space, where it is diagonal, and back-transform before integrating over the velocity field. With the Neumann boundary conditions, the appropriate Fourier basis is the cosine basis, in which the solution to the diffusion equation has the form

$$\rho(\mathbf{r}, t) = \frac{4}{L_x L_y} \sum_{\mathbf{k}} \tilde{\rho}(\mathbf{k}) \cos(k_x x) \cos(k_y y) \exp(-k^2 t), \quad (7)$$

where the sum is over all wave vectors  $\mathbf{k} = (k_x, k_y) = 2\pi(m/L_x, n/L_y)$  with  $m, n$  non-negative integers, and  $\tilde{\rho}(\mathbf{k})$  is the discrete cosine transform of  $\rho(\mathbf{r}, t = 0)$ :

$$\tilde{\rho}(\mathbf{k}) = \frac{1}{4} (\delta_{k_x, 0} + 1) (\delta_{k_y, 0} + 1) \int_0^{L_x} \int_0^{L_y} \rho(\mathbf{r}, 0) \cos(k_x x) \cos(k_y y) dx dy, \quad (8)$$

where  $\delta_{i,j}$  is the Kronecker symbol. The velocity field  $\mathbf{v}$  is then easily calculated from Eqs. (5) and (7) and has components

$$v_x(\mathbf{r}, t) = \frac{\sum_{\mathbf{k}} k_x \tilde{\rho}(\mathbf{k}) \sin(k_x x) \cos(k_y y) \exp(-k^2 t)}{\sum_{\mathbf{k}} \tilde{\rho}(\mathbf{k}) \cos(k_x x) \cos(k_y y) \exp(-k^2 t)}, \quad (9a)$$

$$v_y(\mathbf{r}, t) = \frac{\sum_{\mathbf{k}} k_y \tilde{\rho}(\mathbf{k}) \cos(k_x x) \sin(k_y y) \exp(-k^2 t)}{\sum_{\mathbf{k}} \tilde{\rho}(\mathbf{k}) \cos(k_x x) \cos(k_y y) \exp(-k^2 t)}. \quad (9b)$$

---

<sup>2</sup>We discuss spherical cartograms briefly in Sec. 7.

Equations (8) and (9) can be evaluated rapidly using the fast Fourier transform and its back-transform respectively, both of which in this case run in time of order  $L_x L_y \log(L_x L_y)$ . We then use the resulting velocity field to integrate Eq. (6), which is a nonlinear Volterra equation of the second kind and can be solved numerically by standard methods [5]. In practice it is the Fourier transform that is the time-consuming step of the calculation and with the aid of the fast Fourier transform this step can be performed fast enough that the whole calculation runs to completion in a matter of seconds or at most minutes, even for large and detailed maps.

### 3 Population density function

The description of our method tells, in a sense, only half the story of how to create a cartogram. Before applying this or indeed any method, we need to choose the starting density  $\rho(\mathbf{r})$  for the map. We can, by defining  $\rho(\mathbf{r})$  in different ways, control the properties of the resulting cartogram, including crucially the balance between accurate density equalization and readability.

Population density is not strictly a continuous function, since people are themselves discrete and not continuous. To make a continuous function the population must be binned or coarse-grained at some level. All methods of constructing cartograms require one to do this, and no single accepted standard approach exists. Part of the art of making a good cartogram lies in shrewd decisions about the definition of the population density.

If we choose a very fine level of coarse-graining for the population density, then the high populations in centers such as cities will require substantial local distortions of the map in order to equalize the density. A coarser population density will cause less distortion, resulting in a map with features that are easier to recognize, but will give a less accurate equalization of the population distribution. The most common choice made by others has been to coarse-grain the population at the level of the (usually political) regions of interest. For example, if one were interested in the United States, one might take the population of each state and distribute it uniformly over the area occupied by that state. This method can be used also with our cartogram algorithm

and we give some examples below. But we are not obliged to use it, and in some cases it may be undesirable, since binning at the level of states erases any details of population distribution below the state level.

On the other hand, if we use a finer resolution and allow for density variation within states then not only can the local distortions of the cartogram become severe, but rapidly varying densities can also slow down the numerical calculations. Regions with population density zero are particularly difficult to deal with because the denominator in Eq. (5) becomes zero and hence the velocity is undefined. In our work we circumvent these issues by first adding a small constant to the density to get rid of zero values, and then applying a spatially uniform Gaussian blur to the population density thus:

$$\rho(\mathbf{r}) = \frac{1}{2\pi\sigma^2} \int_0^{L_x} \int_0^{L_y} \rho_{\text{raw}}(\mathbf{r}') \exp\left[-\frac{(\mathbf{r}' - \mathbf{r})^2}{2\sigma^2}\right] dx' dy', \quad (10)$$

where  $\sigma$  is the width of the Gaussian and  $\rho_{\text{raw}}$  is the unblurred density. Varying the width  $\sigma$  of the blurring function is a convenient way to tune the cartogram between accuracy and readability.

This blur can be performed rapidly in Fourier space, where the convolution becomes a simple multiplication. Alternatively, we note that Eq. (10) is equal to the density we would get if we simply allowed  $\rho_{\text{raw}}$  to diffuse for a time  $\frac{\sigma^2}{2}$ , so that we can also use Eq. (7) to calculate the Gaussian blur.

Ultimately the choice of population density function is up to the user of the method, who must decide what particular features are most desirable in his or her application. One advantage of our diffusion-based algorithm is that it is entirely agnostic about this choice; the process of computing the cartogram is decoupled from the calculation of the population density and, hence, is not slanted in favor of one choice or another.

## 4 Applications I: Population cartograms and aggregation

In the remainder of this paper we give several examples of the use of our cartograms, focusing on the United States and using population data from

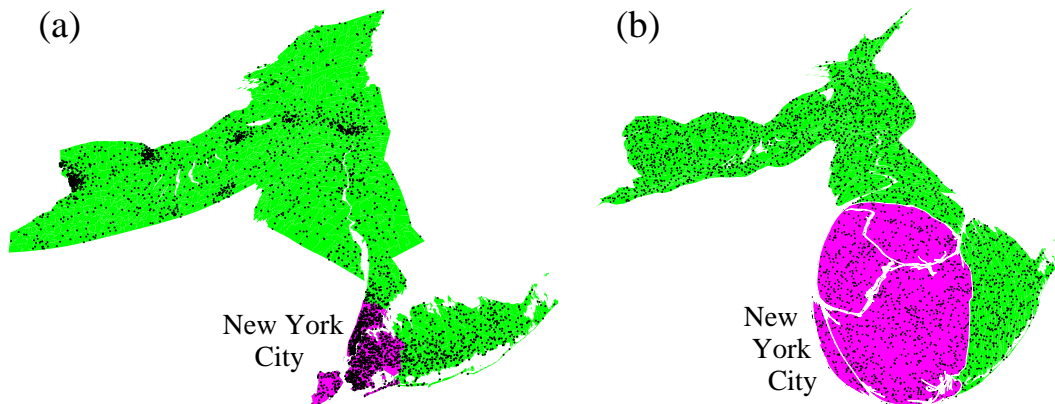


Figure 2: Lung cancer cases among males in the state of New York, 1993-1997, as in Fig. 1(a), but now plotted on population cartograms with (a) a coarse-grained population density with  $\sigma = 50\text{km}$  and (b) a finer-grained population density with  $\sigma = 1\text{km}$ .

the 2000 U.S. Census. First, we reexamine the New York lung cancer map, Fig. 1(a), creating cartograms from population density functions with Gaussian blurs of various widths, as described in the preceding section.<sup>3</sup> In Fig. 2(a), we show the data for cancer cases on a cartogram with only moderate blurring. Although the map is visibly distorted, a reader familiar with the state of New York would still be able to identify different regions because of the shape of the state boundary. The distribution of cancer cases however is still visible “clumped.”

In Fig. 1(b) we use a much finer Gaussian blur, creating a cartogram with better population equalization and significantly greater distortion. Now the virtue of this representation becomes strikingly clear. As the figure shows, when we use a projection that truly equalizes the population density over the map, there is no longer any obvious variation in the distribution of cases over the state—the pattern appears random with more or less the same density of cases everywhere. The shape of the map in Fig. 1(b) does not much resemble the shape of the original any more, but this is the price we pay for equalizing

---

<sup>3</sup>A similar study using a different technique and for a smaller area was carried out by Merrill [6].

the population almost perfectly.

We do not need to rely on eyesight for judging whether the distribution of points in Fig. 1(b) is clustered. There are several statistical methods to test spatial distributions for randomness. A particularly simple measure is the Hopkins statistic  $H$ , a number between 0 and 1 whose expectation value for random point patterns is  $\frac{1}{2}$ . Higher values are a sign of clustering; lower values indicate repulsion between points. Furthermore, it can be shown that the value of the Hopkins statistic on random points is beta-distributed, which allows us to calculate a  $p$ -value—the probability that the observed value of the Hopkins statistic would occur if point position were purely random [7].

Calculating the Hopkins statistic for Fig. 1(a) gives a value of  $H = 0.89 \pm 0.03$  and a  $p$ -value  $< 10^{-16}$ . This is of course hardly surprising since the distribution shows very clear clustering around the major urban centers. But when we perform the same calculation for the points on the cartogram Fig. 2(b) we obtain  $H = 0.50 \pm 0.03$  consistent with a random distribution. Thus, the per capita risk of lung cancer appears, by this calculation, to be the same everywhere. One might imagine that environmental effects such as pollution in big cities could influence cancer rates, but we see no evidence of this. A more careful analysis of course would have to take into account that people might move between the time when they are exposed to a carcinogen and the time when they develop cancer. However, Figure 1(a), despite its impressive clustering, definitely cannot be taken as evidence that there are high-risk regions of New York state for cancer. This finding is consistent with medical evidence that lung cancer is caused by individual behavior rather than environmental causes, with smoking alone responsible for 90% of all cases worldwide [8].

Not all threats to our well-being, however, are uniformly distributed. In Fig. 3(a) we plot each of the 2301 homicides that occurred in the state of California in the year 2001 on an equal-area map, and the map again shows clear clustering around urban areas, particularly the Greater Los Angeles area. Switching once again to a high-resolution population cartogram, Fig. 3(b), we see that the points become more spread out, as before, but this time it is clear that the distribution is far from random. Especially in the southwestern part of Los Angeles the density is clearly higher than average even on the cartogram.

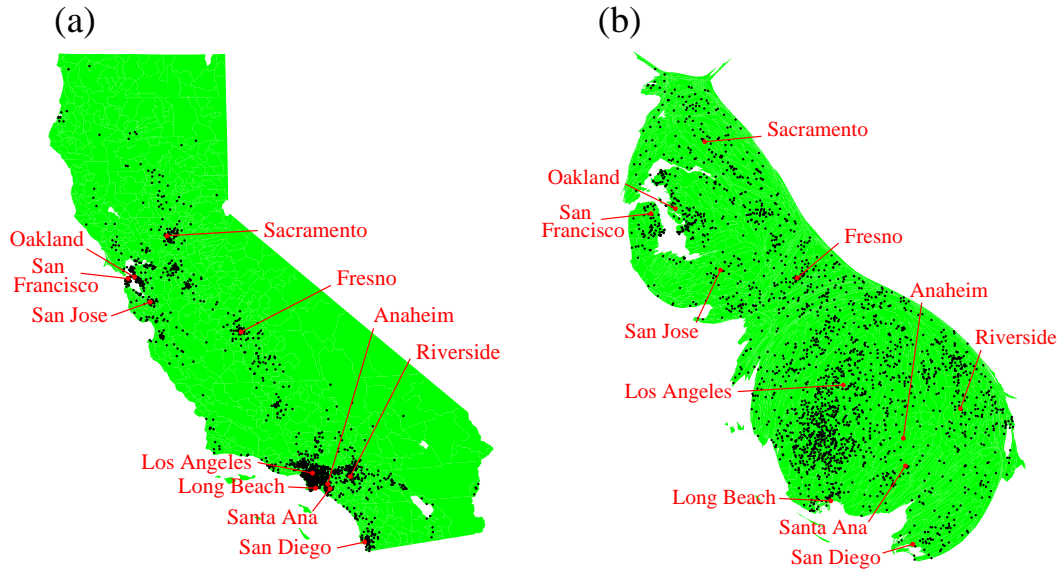


Figure 3: Homicides in California in 2001. (a) Equal-area projection. (b) Population cartogram. Data from the California Department of Health Services.

The Hopkins statistic confirms this impression. Its value of  $0.68 \pm 0.04$  for the cartogram indicates that there is clustering even on the cartogram and the  $p$ -value for complete spatial randomness is below  $10^{-8}$ , meaning the probability that we would get a point pattern such as this purely by chance is below one in a hundred million. Undoubtedly, some parts of the state experience a statistically significant higher number of homicides per capita than others.

For the last example in this section we look at technological rather than social data and analyze the geographic distribution of the Internet in the contiguous United States. The Internet is a network of computers and routers connected by optical fiber. Computers belonging to the same company or organization are typically grouped together into subnetworks called Autonomous Systems (ASes) or routing domains that share a single external routing policy. Here we treat each AS as a single point in geographic space; we have created a map of the Internet using the software tool NetGeo,<sup>4</sup> which can return approximate latitude and longitude for a specified AS. The positions of the 7049

<sup>4</sup><http://www.caida.org/tools/utilities/netgeo>

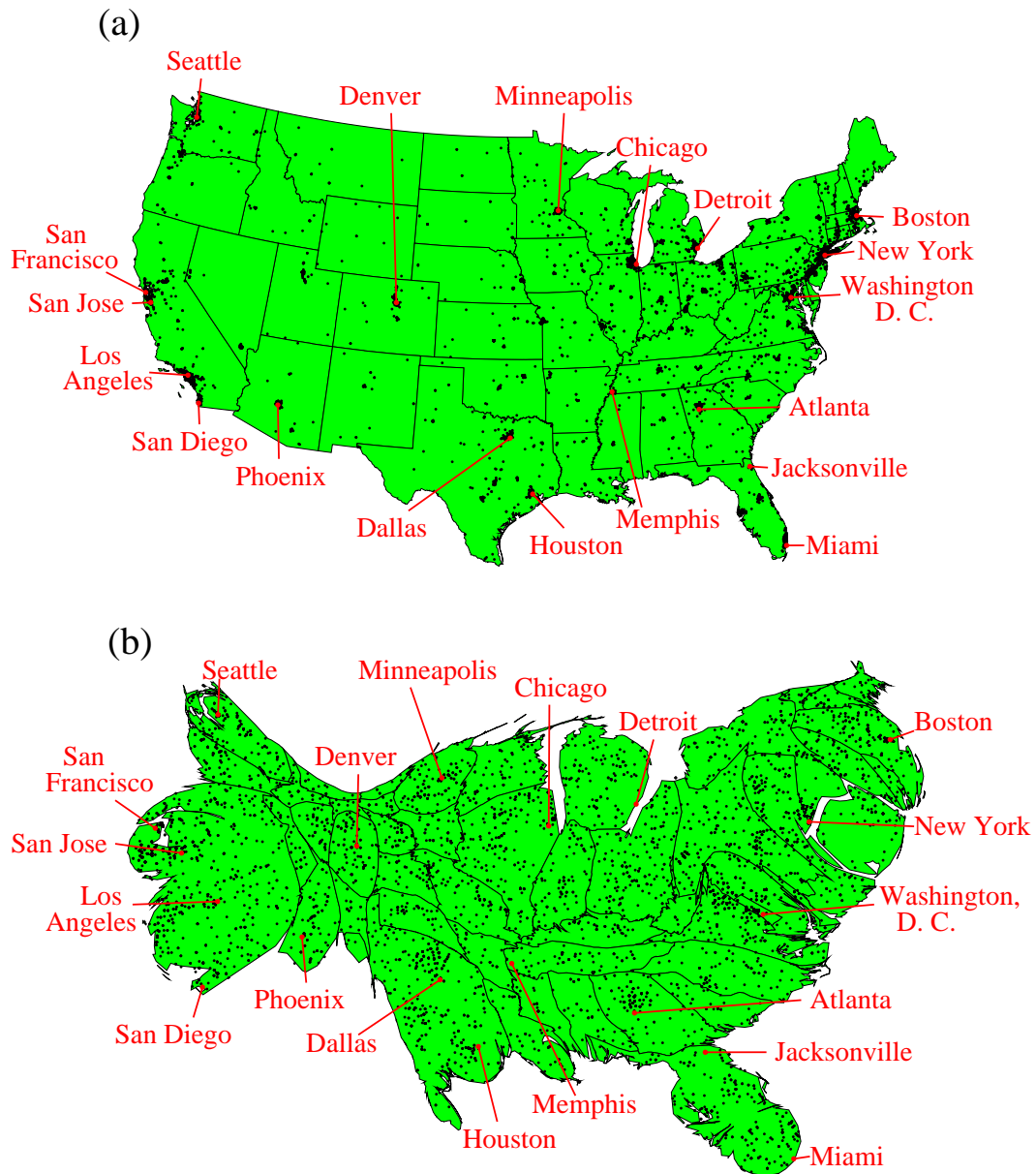


Figure 4: Autonomous systems on the Internet in the contiguous United States (March 2003). (a) Equal-area projection. (b) Population cartogram.

ASes in the lower 48 states in March 2003 is shown in Fig. 4(a).

That ASes on this *equal-area map* appear heavily clustered in cities comes as no surprise since there are more people in the cities. Switching to a car-

togram, Fig. 4(b), we find in this case that, like the homicides, the ASes become more uniform, but are still concentrated around the cities. Some urban areas appear particularly dense, such as Silicon Valley (west of San Jose), Manhattan (New York City), or Washington, DC. Other cities, by contrast, appear to have no more ASes per capita than average—for example, Detroit, Memphis, and Jacksonville. The Hopkins statistic for the distribution on the cartogram takes a value of  $H = 0.80 \pm 0.04$ , and the random distribution is firmly ruled out (the  $p$ -value is  $< 10^{-16}$ ). In the early days of the Internet it was often claimed that geographic position would become unimportant thanks to high-speed data transmission and easy access to information from everywhere. Apparently, this has not happened.

## 5 Applications II: Cartograms based on other density functions

The cartograms shown so far have all been based on human population density, which is certainly the most common type of cartogram. Other types, however, are also possible and we give some examples in this section.

For our first example we examine the usage and production of energy in the United States. Each year, the US Energy Information Administration estimates each state's total energy consumption, including electricity, coal, gas, petroleum, wood, and alternative energy sources [9]. For instance, in the year 2000 the United States consumed a total of 98 quadrillion British thermal units of energy. The use of energy varies greatly between the states, with Texas, for example, consuming 70 times as much energy as Vermont.

In Fig. 5(a) we show a cartogram in which states are scaled according to their total energy consumption during the year 2000. The cartogram appears quite similar to the population cartogram in Fig. 4(b), indicating that energy consumption per capita is roughly the same in most parts of the country. On closer inspection one might detect that the biggest state in Fig. 4(b), California, has been overtaken in Fig. 5(a) by what was formerly the second biggest state, Texas. New York and Florida have also become smaller, Pennsylvania and

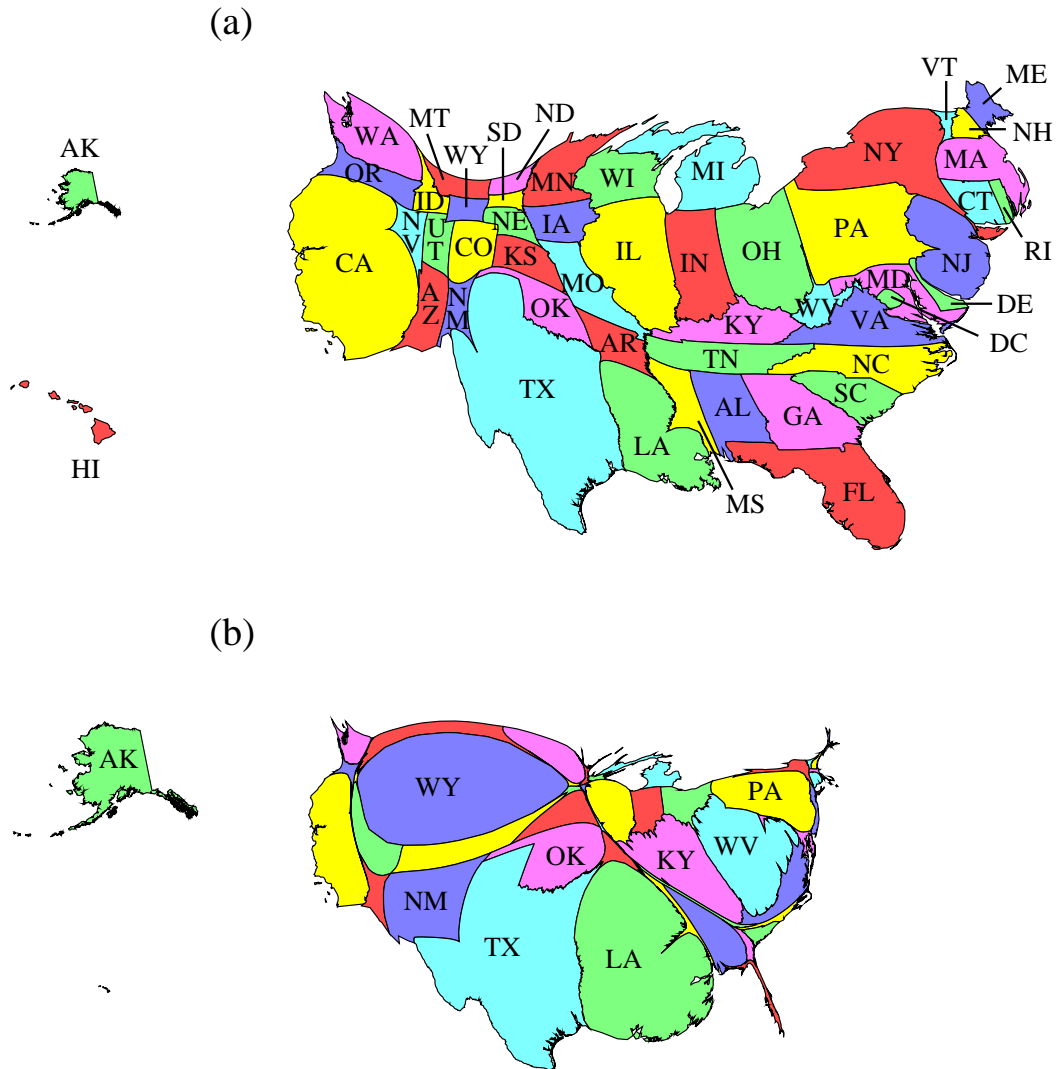


Figure 5: (a) A cartogram of the United States in which the sizes of states are proportional to their total energy consumption. (b) A similar cartogram for energy production. States are the same color in (a) and (b).

Louisiana larger, but all in all the changes are relatively minor—population density explains energy consumption quite well.

But now look at Fig. 5(b), which shows total energy *production* by state, again from figures compiled by the Energy Information Administration for

the year 2000 and including crude oil, gas, and coal as well as electricity not generated from fossil fuels [10]. This cartogram gives a very different perspective on the country. A small number of states, most notably Texas, Louisiana, and Wyoming, dominate the country's energy production, the first two because of their wealth in oil and gas, the third because of its abundance of coal. Total US energy production is 61 quadrillion British thermal units, which is only 62% of consumption—the difference is made up of imported energy—so the total area of Fig. 5(b) is smaller than that of Fig. 5(a) by the same factor. Figures 5(a) and (b) together highlight the substantial redistribution of energy from producer to consumer in the United States.

For our second example of a cartogram not based on population density we examine the media attention paid to different parts of the country. Anyone who reads or watches the news in the United States (and similar observations probably apply in other countries as well) will have noticed that the geographical distribution of news stories is not uniform. Even allowing for population, a few cities, notably New York and Washington, DC, get a surprisingly large fraction of the attention while other places get little. Apparently some locations loom larger in our mental map of the nation than others, at least as presented by the major media. We can turn this qualitative idea into a real map using our cartogram method.

We have taken about 72 000 newswire stories from November 1994 to April 1998,<sup>5</sup> and extracted from each the “dateline,” a line at the head of the story that gives the date and the location that is the main focus of the story. Binning these locations by state, we then produce a map in which the sizes of the US states are proportional to the number of stories concerning that state over the time interval in question. The result is shown in Fig. 6.

The stories are highly unevenly distributed. New York City alone contributes 20 000 stories to the corpus, largely because of the preponderance of stories about the financial markets, and Washington, DC another 10 000,

---

<sup>5</sup>Data from the Associated Press Worldstream wire service, compiled and distributed on CD-ROM by the Linguistic Data Consortium (North American News Text Supplement 1998).

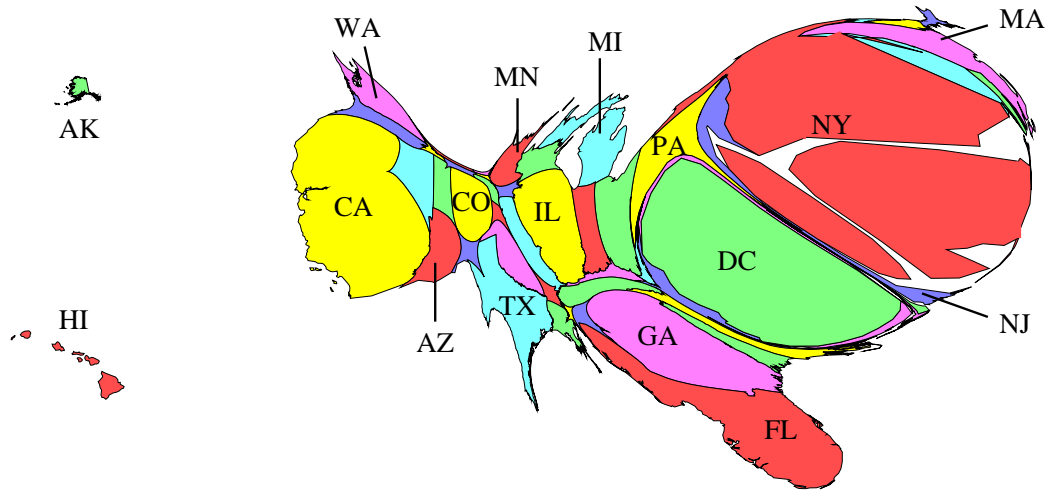


Figure 6: Cartogram in which the sizes of states are proportional to the frequency of their appearance in news stories. States are the same color as in Fig. 5.

largely political stories. We chose to bin by state to avoid large distortions around the cities that are the focus of most news stories. We made one exception however: since New York City had far more hits than any other location including the rest of the state of New York (which had around 1000), we split New York State into two regions, one for the greater New York City area and another for the rest of the state.

The cartogram offers a dramatic depiction of the distribution of US news stories. The map is highly distorted because the patterns of reporting show such extreme variation. Washington, DC, for instance, which normally would be virtually invisible on a map of this scale, becomes the second largest “state” in the union. (The District of Columbia is not, technically, a state.) People frequently overestimate the size of the northeastern part of the United States by comparison with the middle and western states, and this map may give us a clue as to why. Perhaps people’s mental image of the United States is not really an inaccurate one; it is simply based on things other than geographical area, such as the attention regions receive in the media.

Numerous other possible applications of cartograms come readily to mind, such as visualizations of gross regional products, numbers of people belong-

ing to certain ethnic groups, sales of consumer goods, and so forth. Diffusion cartograms might also have applications outside geography. One possibility is the creation of a homunculus, a representation of the human body in which each bodily part is scaled in proportion to the size of the brain region devoted to it [11]. Such representations are usually constructed as two-dimensional plots, but there is no reason in theory why one could not create a fully three-dimensional homunculus; the diffusion process is easily generalized to any number of dimensions.

## 6 Performance of the algorithm

An important consideration with any method for producing cartograms is efficiency. In many cases one would like to create cartograms interactively for data exploration, which means that program run times for producing them should be limited to seconds, or at most a few minutes for the most complex cartograms such as the larger country-sized ones shown above. In this section we provide some figures on run times and analysis of the efficiency of our cartogram method.

We have implemented our algorithm as a C program and it is this implementation that we analyze here. (No doubt faster implementations than ours are possible, given time and effort, but we believe ours to give a good general indication of the speeds attainable.) We analyze the performance of the program in calculating a cartogram of the lower 48 states and the District of Columbia with each region scaled according to population.

The program goes through the following steps in creating the cartogram. First, the polygons making up the regions of the input map are read from ASCII files, along with data on the population of each region. Then, a fine square grid is created and filled with the initial density distribution. The grid spacing has to be chosen such that the smallest polygon is covered by at least a few grid points. For the present example we chose a  $1024 \times 512$  grid, which is adequate to resolve the smallest region, the District of Columbia. The program then evaluates the cartogram transformation for each grid point by solving the diffusion equation as outlined in Sec. 2. The positions of the vertices of each

polygon are calculated by piecewise bilinear transformations from the points of the distorted grid.<sup>6</sup> For this example our program runs to completion within  $3\frac{1}{2}$  minutes on a standard desktop computer with a 2.8GHz Intel Pentium IV processor. Total memory used is 22MB.

Another important measure is the accuracy of the algorithm. How precisely are the final areas proportional to population? We measure the fractional error in each region's area by calculating the quantity

$$\text{relative error} = \frac{\text{area of state on cartogram} \times \text{total population of all states}}{\text{total area of all states on map} \times \text{population of state}} - 1. \quad (11)$$

The results are shown as the red bars in Fig. 7. Most states are within  $\pm 10\%$  of their target value, with the exception of Washington, DC, and Rhode Island, which are too small, and Vermont and West Virginia, which are too big. The inaccuracies are caused partly by sampling the density on a finite grid and partly by approximations made by the integrator routine. For most applications these errors are probably acceptable. On the input map the densities vary by more than a factor of 1600 between the densest region, Washington, DC, and the sparsest, Wyoming. On the cartogram the extreme densities—now Washington, DC, and West Virginia—only differ by a factor of about 2, or almost three orders of magnitude less.

However, if the errors are a major concern there is a simple way to improve the result, namely running the algorithm again starting from the cartogram produced by the first run. The time taken is the same as before, but the area errors are now reduced to less than 3.5% in all cases (the green bars in Fig. 7) which is certainly much less than can be detected by eye. If even higher accuracy is needed one can of course run the algorithm as many times as needed. Alternatively, one could make the initial square grid finer from the start at the expense of longer run-times. For an  $L_x \times L_y$  grid the time needed for a single run scales as  $L_x L_y \log(L_x L_y)$ , the bottleneck being the fast

---

<sup>6</sup>It would be entirely possible—and in some cases quicker—to transform the polygon vertices separately using the diffusion equation, but the grid-based method described here is simpler and more general and gives results essentially as good; the grid is fine enough that the errors introduced by the interpolation are small.

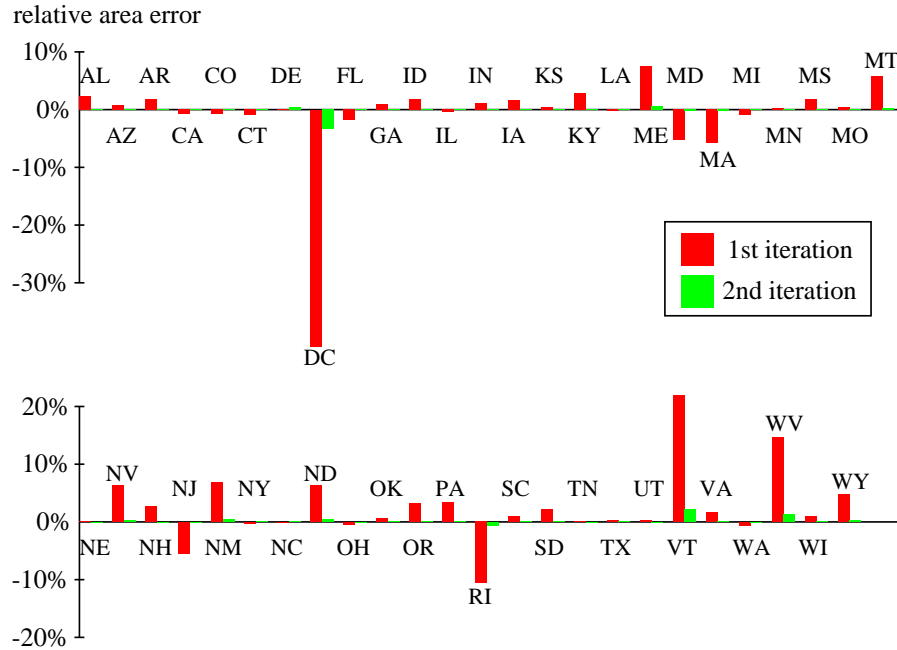


Figure 7: Relative area errors on a population cartogram of the lower 48 states and Washington, DC, after applying the cartogram program.

Fourier transform. The memory use grows as  $L_x L_y$ . Memory is not likely to be a problem on current computers for maps of any reasonable size. We have without difficulty carried out computations on lattices of size up to  $4096 \times 2048$ .

Off-shore islands and donut shaped regions are treated correctly by our method; their topology will be strictly preserved. If, however, the map consists of several non-contiguous regions scattered over a wide area with a lot of empty space in between, covering all of the map with one big grid can be wasteful. For example, on an accurate map of all fifty states in the USA, Alaska extends so far to the north and Hawaii so far to the west of the American continent that calculating the cartogram on a grid wide enough to reach the remotest parts of the country would be very wasteful. We would in particular spend a large fraction of our effort on points in the middle of the Pacific Ocean between California and Hawaii, which are irrelevant for most purposes.

Conventionally, map makers move Alaska and Hawaii closer to the contiguous USA to fit them on one map, but this is a rather poor choice as input

to our cartogram program because moving them closer to the lower 48 states can cause their diffusion patterns to interact with those of the lower 48, influencing the final shape of the cartogram.<sup>7</sup> (The areas of the states would still be correct, but their shapes would be distorted.) A better solution is to construct separate cartograms for Alaska and Hawaii, and then afterward place them next to the cartogram for the continental USA in the traditional fashion. Some care must be taken to make sure the population scale of the different cartograms matches correctly. The cartograms in Figs. 5 and 6 were constructed in this manner.

## 7 Discussion and conclusions

In this paper we have described a new general method for constructing density-equalizing projections or cartograms, which provide an invaluable tool for the presentation and analysis of geographic data. Our method is simpler than many earlier methods, allowing for rapid calculations, while generating accurate and readable maps. The method allows its users to choose their own balance between good density equalization and low distortion of map regions, making it flexible enough for a wide variety of applications. We have presented a number of examples of the use of our cartograms to represent human data.

We have implemented our method as a C program which is available from our web site.<sup>8</sup> Directly embedding the algorithm as a function in GIS software packages should also be straightforward. For even the most complex examples, the program achieves good density-equalization on the time scale of a few minutes with current computing resources.

One interesting direction for future research is the creation of cartograms in spaces that are not flat. Here we have assumed that our mapped space is flat,

---

<sup>7</sup>Islands just off the coast, like Long Island, will of course influence diffusion on the mainland too, but this is correct because these islands really are in the “neighborhood” and their influence should be felt. The high population of Brooklyn and Queens on Long Island for example should expand and repel the mainland as in Fig. 2, thereby preserving the topology of map.

<sup>8</sup><http://www-personal.umich.edu/~mgastner>

but this is never strictly true since the surface of the Earth is curved. Even for an area as large as the contiguous United States it is usually legitimate to neglect curvature when a suitable projection is used for the input map (such as the Albers conic projection used here). For a larger area—a cartogram of the entire world, for instance—this would no longer be possible. In that case we would have to solve the diffusion equation (4) on the surface of the sphere in spherical coordinates:

$$\frac{1}{\sin \theta} \frac{\partial}{\partial \theta} \left( \sin \theta \frac{\partial \rho}{\partial \theta} \right) + \frac{1}{\sin^2 \theta} \frac{\partial^2 \rho}{\partial \phi^2} = \frac{\partial \rho}{\partial t}. \quad (12)$$

The solution can be expressed in terms of spherical harmonics  $Y_{lm}(\theta, \phi)$  thus:

$$\rho(\theta, \phi, t) = \sum_{l=0}^{\infty} \sum_{m=-l}^l \tilde{\rho}_{lm} Y_{lm}(\theta, \phi) \exp[-l(l+1)t] \quad (13)$$

where

$$\tilde{\rho}_{lm} = \int Y_{lm}^*(\theta, \phi) \rho(\theta, \phi, t=0) d\Omega. \quad (14)$$

As in the Cartesian case we can now use Eq. (5) to solve for the velocities

$$\begin{aligned} v_{\theta}(\theta, \phi, t) &= -\frac{1}{\rho} \frac{\partial \rho}{\partial \theta} \\ &= \frac{\sum_{l=0}^{\infty} \sum_{m=-l+1}^l \sqrt{l(l+1) - m(m-1)} \tilde{\rho}_{lm} Y_{l,m-1}(\theta, \phi) e^{i\phi} e^{-l(l+1)t}}{2 \sum_{l=0}^{\infty} \sum_{m=-l}^l \tilde{\rho}_{lm} Y_{lm}(\theta, \phi) \exp[-l(l+1)t]} \\ &\quad - \frac{\sum_{l=0}^{\infty} \sum_{m=l}^{l-1} \sqrt{l(l+1) - m(m+1)} \tilde{\rho}_{lm} Y_{l,m+1}(\theta, \phi) e^{-i\phi} e^{-l(l+1)t}}{2 \sum_{l=0}^{\infty} \sum_{m=-l}^l \tilde{\rho}_{lm} Y_{lm}(\theta, \phi) e^{-l(l+1)t}}, \\ v_{\phi}(\theta, \phi, t) &= -\frac{1}{\rho \sin \theta} \frac{\partial \rho}{\partial \phi} \\ &= -i \frac{\sum_{l=0}^{\infty} \sum_{m=-l}^l m \tilde{\rho}_{lm} Y_{lm}(\theta, \phi)}{\sin \theta \sum_{l=0}^{\infty} \sum_{m=-l}^l \tilde{\rho}_{lm} Y_{lm}(\theta, \phi) e^{-l(l+1)t}}. \end{aligned} \quad (15)$$

To solve Eqs. (13), (14), and (15) efficiently we need the equivalent of the fast Fourier forward and backward transforms for spherical harmonics. Although such transforms exist, implementations are far from trivial and a current field of research [12].

## Acknowledgments

The authors would like to thank the staff of the University of Michigan's Numeric and Spatial Data Services for their help with the geographic data, and Dragomir Radev for useful discussions about the geographic distribution of news messages. This work was funded in part by the National Science Foundation under grants DMS-0234188 and DMS-0405348 and by the James S. McDonnell Foundation.

## References

- [1] S. M. Guseyn-Zade and V. S. Tikunov, "Analog methods in the compilation of areal transformed images," *Mapping Sciences and Remote Sensing*, vol. 31, pp. 49–65, 1994.
- [2] D. Dorling, "Area cartograms: Their use and creation," *Concepts and Techniques in Modern Geography (CATMOG)*, vol. 59, 1996.
- [3] B. D. Dent, *Cartography: Thematic Map Design*. Boston: WCB/McGraw-Hill, 5th ed., 1999.
- [4] W. Tobler, "Thirty five years of computer cartograms," *Annals of the Association of American Geographers*, vol. 94, pp. 58–73, 2004.
- [5] W. H. Press, S. A. Teukolsky, W. T. Vetterling, and B. P. Flannery, *Numerical Recipes in C*. Cambridge: Cambridge University Press, 1992.
- [6] D. W. Merrill, "Use of a density equalizing map projection in analysing childhood cancer in four California counties," *Statistics in Medicine*, vol. 20, pp. 1499–1513, 2001.
- [7] B. Hopkins, "A new method for determining the type of distribution of plant individuals," *Annals of Botany*, vol. 18, pp. 213–227, 1954. Appendix by J. G. Skellam.
- [8] A. Spira, J. Beane, V. Shah, G. Liu, F. Schembri, X. Yang, J. Palma, and J. S. Brody, "Effects of cigarette smoke on the human airway epithelial

- cell transcriptome,” *Proceedings of the National Academy of Sciences of the United States of America*, vol. 101, pp. 10143–10148, 2004.
- [9] “State Energy Data Report 2000,” technical report, Energy Information Administration, Office of Energy Markets and End Use, U.S. Department of Energy, Washington, DC.
- [10] [http://www.eia.doe.gov/emeu/states/2000StateEnergy\\_Sep2003.xls](http://www.eia.doe.gov/emeu/states/2000StateEnergy_Sep2003.xls).
- [11] J. Mitchell, ed., *The Random House Encyclopedia*, p. 667. New York: Random House, 3rd ed., 1990.
- [12] D. M. Healy, D. N. Rockmore, P. J. Kostelec, and S. Moore, “FFTs for the 2-sphere—improvements and variations,” *Journal of Fourier Analysis and Applications*, vol. 9, pp. 341–385, 2003.